Topological Phase Transition in non-Hermitian Quasicrystals

S. Longhi*
Dipartimento di Fisica - Politecnico di Milano, Piazza Leonardo da Vinci 32, 20133 Milan, Italy
and Istituto di Fotonica e Nanotecnologie - Consiglio Nazionale delle Ricerche,
Piazza Leonardo da Vinci 32, 20133 Milan, Italy

(Received 10 December 2018; published 11 June 2019)

The discovery of topological phases in non-Hermitian open classical and quantum systems challenges our current understanding of topological order. Non-Hermitian systems exhibit unique features with no counterparts in topological Hermitian models, such as failure of the conventional bulk-boundary correspondence and non-Hermitian skin effect. Advances in the understanding of the topological properties of non-Hermitian lattices with translational invariance have been reported in several recent studies; however little is known about non-Hermitian quasicrystals. Here we disclose topological phases in a quasicrystal with parity-time ($\mathcal{PT}$) symmetry, described by a non-Hermitian extension of the Aubry-André-Harper model. It is shown that the metal-insulating phase transition, observed at the $\mathcal{PT}$ symmetry breaking point, is of topological nature and can be expressed in terms of a winding number. A photonic realization of a non-Hermitian quasicrystal is also suggested.

DOI: 10.1103/PhysRevLett.122.237601

Introduction.—The discovery of topological phases of matter has introduced a major twist in condensed matter physics [1,2] with great impact in other areas of physics, such as photonics, atom optics, acoustics, and mechanics [3–8]. Topological band theory classifies Hermitian topological systems depending on their dimensionality and symmetries [9,10]. The bulk topological invariants are uniquely reflected in robust edge states localized at open boundaries. The ability to engineer non-Hermitian Hamiltonians, demonstrated in a series of recent experiments [11–17], and the related observation of unconventional topological boundary modes sparked a great interest to extend topological band theory to open systems [18–40]. Striking features are the failure of the conventional bulk-boundary correspondence [27,31,35,37–40], eigenstate condensation [30,31], the non-Hermitian *skin effect* [33,37,38], and the sensitivity of the bulk spectra on boundary conditions [19,36,39–41]. Most previous studies have been concerned with crystals; however, little is known about the topological properties of non-Hermitian quasicrystals. Quasicrystals (QCs) constitute an intermediate phase between fully periodic lattices and fully disordered media, showing a long-range order but no periodicity [42,43]. A paradigmatic model of a one-dimensional (1D) QC is provided by the Aubry-André-Harper (AAH) Hamiltonian [43–45], which is known to show a metal-insulator phase transition [44–46]. In the Hermitian case, the AAH Hamiltonian is topologically nontrivial because it can be mapped into a two-dimensional quantum Hall system on a square lattice [47–50]. A few recent studies have considered some non-Hermitian extensions of the AAH model [51–56], mainly with a commensurate potential and with open boundary conditions. Such numerical studies investigated how gain and loss distributions affect edge states and parity-time ($\mathcal{PT}$) symmetry breaking [51–53,55], the Hofstadter butterfly spectrum [52], and the localization properties of eigenstates [54,56]. However, so far there is not any evidence of *topological* phases and topological phase transitions in non-Hermitian QCs.

The aim of this Letter it to disclose topological phases in non-Hermitian quasicrystals, described by a $\mathcal{PT}$-symmetric extension of the AAH model. The main result is that the localization-delocalization phase transition, observed at the $\mathcal{PT}$ symmetry breaking point in the thermodynamic limit, is of topological nature and can be expressed in terms of a winding number which characterizes the two distinct phases of the system. A photonic realization of the topological phase transition is proposed, which is based on the spectral properties of mode-locked lasers with an intracavity etalon.

Non-Hermitian Aubry-André-Harper model.—The tight-binding Hamiltonian of the AAH model, describing the hopping dynamics on a 1D lattice with an incommensurate potential, reads [42–46]

$$H(\varphi)\psi_n = J(\psi_{n+1} + \psi_{n-1}) + V_n\psi_n \tag{1}$$

for the occupation amplitudes ψ_n at the various sites of the lattice, where J is the hopping rate,

$$V_n = V\cos(2\pi\alpha n + \varphi) \tag{2}$$

is the onsite potential, V and φ are the amplitude and phase of the potential, and α is irrational for a QC. Here we consider

a non-Hermitian extension of the AAH Hamiltonian by complexification of the potential phase φ, i.e., we assume

$$\varphi = \theta + ih, \tag{3}$$

which yields

$$V_n = V\cos(2\pi\alpha n + \theta + ih) \tag{4}$$

for the incommensurate on-site potential. Note that for $\theta = 0$ one has $V_{-n} = -V_n^*$ and $H(\varphi)$ is $\mathcal{PT}$ symmetric. In the Hermitian limit $h = 0$, H is an almost Mathieu operator which shows very rich and subtle spectral features, which have been extensively investigated in the mathematical literature [57,58]. Roughly speaking, for irrational α the Hamiltonian H shows a metal-insulator phase transition: for $V < 2J$ all eigenstates are delocalized (metallic phase) and the spectrum is independent of θ, whereas for $V > 2J$ all eigenstates are localized (insulating phase) with an inverse localization length (Lyapunov exponent) independent of the eigenenergy and given by $\gamma = \log(V/2J)$ [44]. Here we are interested in studying the bulk properties of H with complex phase φ and to disclose topological phases in the thermodynamic limit $L \to \infty$ of number L of lattice sites. Since any irrational number α can be approximated by a sequence of rational numbers p_n/q_n with p_n, q_n prime integers and p_n, $q_n \to \infty$ as $n \to \infty$ [59], in numerical simulations one can assume as usual a finite (yet arbitrarily large) number of sites $L = q_n$ on a ring with periodic boundary conditions $\psi_{n+L} = \psi_n$. Clearly, in an ordinary crystal (α rational) in the thermodynamic limit $L \to \infty$ a large number of unit cells are reproduced inside the ring; however for irrational α there is not any unit cell that is exactly reproduced inside the ring.

Topological phases, symmetry breaking, and metal-insulator transition.—Topological properties of 1D superlattices and QCs in Hermitian models have attracted great interest recently [47,48,50,60–66]. In particular, the connection between the Hermitian AAH model and the two-dimensional quantum Hall (Harper-Hofstadter) system [47,64], when the phase θ is considered as a synthetic additional dimension, has lead to the demonstration of topological pumping [67] of edge states in photonic QCs [47]. However, the possibility that topological properties of 1D QCs can emerge from higher dimensions is a matter of debate [46,60,61,64]. In a recent work [37], Gong and co-workers introduced a topological classification of non-Hermitian Hamiltonians that can be safely applied to systems with broken translational invariance. Following such an approach, we consider here the case $V < 2J$, corresponding to the delocalized phase in the Hermitian limit $h = 0$, and assume the imaginary phase term h as the control (deformation) parameter of the Hamiltonian $H(\varphi) = H(\theta, h)$, where the dependence of H on θ and h is defined by Eqs. (1)–(3). For $h = 0$, the spectrum of $H(\theta)$ is absolutely continuous, has a Cantor-set structure with a dense set of gaps and is independent of θ [57,58]. For example, when α is the inverse of the golden mean, $\alpha = (\sqrt{5}-1)/2$, the spectrum consists of mainly three "bands," which again consist of three subbands and so forth [see upper panel in Fig. 1(a)]. Let E_B be a base energy which is not an eigenenergy of H but it is assumed to be embedded in a small gap of the Cantor set. Let us then introduce a winding number $w = w(h)$ as follows:

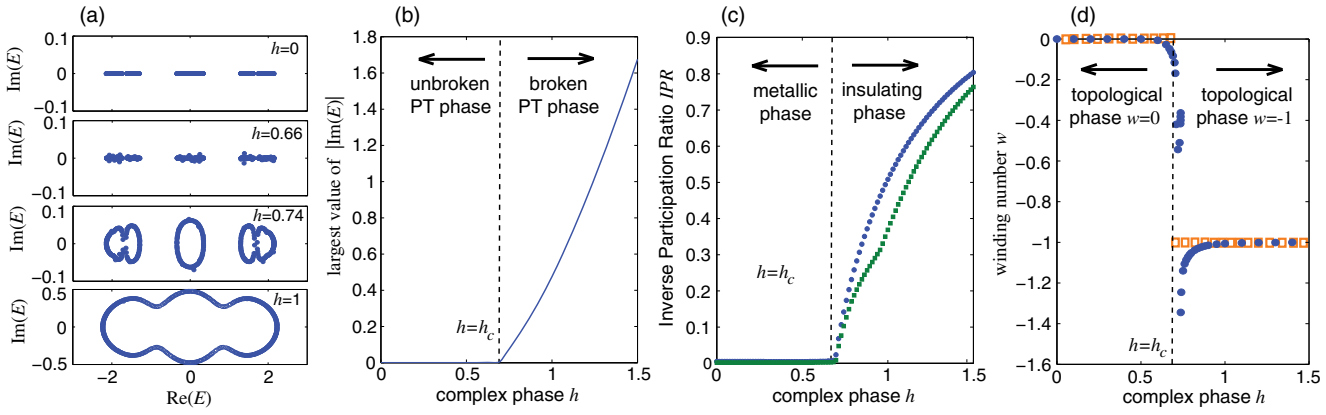

FIG. 1. Topological phase transition in the non-Hermitian Aubry-André-Harper Hamiltonian $H(\theta, h)$ for $J = V = 1$, $\alpha = (\sqrt{5}-1)/2$. Periodic boundary conditions are assumed on a lattice with $L = 610$ sites. (a) Energy spectrum E of H for $\theta = 0$ and for a few increasing values of the complex phase h. (b) Behavior of the largest value of $|\mathrm{Im}(E)|$ vs h for $\theta = 0$. The dashed vertical curve corresponds to the critical value $h_c = \log(2J/V) \simeq 0.6931$ predicted in the thermodynamic limit $L \to \infty$. (c) Numerically computed behavior of the largest and smallest values of inverse participation ratio IPR of eigenstates vs h. (d) Behavior of the winding number w vs h for E_B as computed using Eq. (5) (circles) and Eq. (S-12) given in the Supplemental Material [68] (squares). The base energy E_B used to compute the winding number w is $E_B = 0$. The value of w does not change if the base energy E_B is varied, provided that it remains embedded in the central band of the Cantor set of H at $h = 0$.

$$w(h) = \lim_{L\to\infty} \frac{1}{2\pi i} \int_0^{2\pi} d\theta \frac{\partial}{\partial\theta} \log\det\left\{H\left(\frac{\theta}{L}, h\right) - E_B\right\}. \tag{5}$$

The winding number w counts the number of times the complex spectral trajectory encircles the base point E_B when the real phase θ varies from zero to 2π [37]. As shown in the Supplemental Material [68], $w = w(h)$ does not depend on E_B, is quantized, and can take only two values depending on the strength of the non-Hermitian phase h

$$w = \begin{cases} 0 & h < h_c \\ -1 & h > h_c, \end{cases} \tag{6}$$

where the critical value h_c is given by

$$h_c = \log\left(\frac{2J}{V}\right). \tag{7}$$

This shows that there are two distinct topological phases of H. The two phases correspond to entirely delocalized eigenstates and real energy spectrum (unbroken $\mathcal{PT}$ phase) for $w = 0$, and to entirely localized eigenstates and complex energy spectrum (broken $\mathcal{PT}$ phase) for $w = -1$. Such a result thus shows that the localization and symmetry-breaking phase transitions at $h = h_c$ are of topological nature. The detailed proof of the above statements is given in the Supplemental Material [68]. Here we just briefly outline the main two steps of the proof. As a first step, by a similarity transformation the Hamiltonian $H(\theta, h)$ is connected to the Hatano-Nelson model [18,19,21] with incommensurate potential, and the localization properties of the eigenstates of H for $h \neq 0$ are thus determined from those of the AAH model in the Hermitian limit $h = 0$ (Sec. S.1 in Ref. [68]). This also entails that the non-Hermitian delocalization-localization phase transition at $h = h_c$ coincides with the $\mathcal{PT}$ symmetry breaking phase transition in the thermodynamic limit (the energy spectrum is entirely real in the delocalized phase, while it becomes complex in the localized phase). As a second step, the topological nature of the phase transition is demonstrated by direct computation of the winding number w (Sec. S.-2 in Ref. [68]), which involves some mathematical steps and a result derived by Thouless [69] that relates the localization length of eigenstates and the density of states. To exemplify and check the validity of the analytical results, we performed numerical diagonalization analysis of the matrix Hamiltonian H by varying the non-Hermitian phase h assuming $\alpha = (\sqrt{5}-1)/2$, $L = 610$ (corresponding to $\alpha L \simeq 377$), $J = V = 1$, and periodic boundary conditions. The localization of eigenstates is measured by the inverse of the participation ratio $\mathrm{IPR} = \sum_n |\psi_n|^4 / (\sum_n |\psi_n|^2)^2$, with $\mathrm{IPR} \simeq 1/L \simeq 0$ for a delocalized state and $\mathrm{IPR} \simeq 1$ for a fully localized state. Figure 1(a) shows a few examples of the energy spectrum E of H for a few increasing values of the non-Hermitian phase h, whereas Fig. 1(b) shows the behavior of the largest value of $|\mathrm{Im}(E)|$ vs h. A rather abrupt increase of $\max\{|\mathrm{Im}(E)|\}$ from zero is clearly observed near $h = h_c \simeq 0.6931$, corresponding to the critical value of the complex phase predicted by the theoretical analysis [Eq. (7)]. The behavior of the IPR vs h, for the eigenstates with either the largest or smallest IPR, is depicted in Fig. 1(c). Clearly, according to the theoretical analysis the critical value $h = h_c$ separates the metal and insulating phases. The topological nature of the phase transition is illustrated in Fig. 1(d), where the winding number w vs h is numerically computed using Eq. (5). Note that contrary to the rather general result of Ref. [37], the trivial topological phase $w = 0$ corresponds here to all eigenstates being delocalized (rather than localized as in Ref. [37]). Such a seemingly inconsistency can be resolved by observing that, as shown in Ref. [68], the non-Hermitian AAH Hamiltonian in the infinitely extended lattice limit can be transformed into the Hatano-Nelson Hamiltonian with incommensurate disorder by a similarity transformation, and that in such a transformation the metal and insulating phases are reversed. The winding number w describes a bulk property of the system; however in our model it is not useful to predict edge states, i.e., to state a bulk-boundary correspondence like in Ref. [37]. Numerical results show that a number of edge states can arise, either at the left or right boundaries, in a lattice with open boundary conditions and in the metallic phase, where w assumes the trivial value $w = 0$ (see Fig. S1 in Ref. [68]). The number of edge states sensitively depends on h. Since edge states correspond rather generally to eigenstates with complex energies, the $\mathcal{PT}$ symmetric phase is fragile in a system with open boundaries, as already noticed in previous works [51–53]. Finally, we note that, while the AAH and Nelson-Hatano Hamiltonians are related one another by a similarity transformation, the non-Hermitian skin effect observed in the latter model, i.e., the shrinking of all bulk states into one edge of the lattice [35], is not found in the AAH model.

Non-Hermitian photonic quasicrystal.—An interesting case is obtained in the double limit $h \to \infty$, $V \to 0$ with $V\exp(h) \to 2V_0$ finite, corresponding to the incommensurate potential $V_n = V_0 \exp(-2\pi i\alpha n - i\theta)$ in Eq. (1). In this case, assuming V_0 as the control parameter of the Hamiltonian, according to Eq. (7) the topological phase transition is attained as V_0 is increased above the critical value $V_{0c} = J$. A simple photonic system that realizes a complex QC of this kind, and thus showing a non-Hermitian topological phase transition, is provided by a frequency-modulated (FM) mode-locked laser [70,71]. Mode-locked lasers are routinely used to generate ultrashort optical pulses [72] and are known to provide experimentally accessible systems to observe phase transitions in their spectrum [73–76]. A schematic of a mode-locked laser that realizes a non-Hermitian QC is

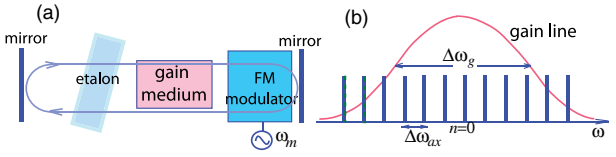

FIG. 2. Non-Hermitian photonic QC. (a) Schematic of the FM mode-locked laser. (b) The axial cavity modes of the laser cavity (vertical lines), coupled by the phase modulator, realize a 1D tight-binding lattice in the spectral domain. The low-finesse etalon introduces an incommensurate complex potential on the lattice.

shown in Fig. 2(a). It consists of a standard Fabry-Perot laser cavity with axial modes spaced by $\Delta\omega_{ax}$ and with an intracavity phase modulator driven at frequency $\omega_m = \Delta\omega_{\rm ax}$. The gain medium is provided by a homogeneously broadened active material with a slow relaxation dynamics and wide gain bandwidth $\Delta\omega_g \gg \Delta\omega_{\rm ax}$ [70]. The spectral axial modes with amplitudes ψ_n realize a 1D lattice in the spectral domain [Fig. 2(b)]. The phase modulator, impressing a time-dependent phase $\Delta\phi(t) = \Delta_{\rm FM}\cos(\omega_m t)$ to the transmitted light field, couples the spectral modes with a hopping rate $J = \Delta_{\rm FM}/2$. A synthetic complex potential $V_n = V_0\exp(2\pi i\alpha n + i\theta)$ on the lattice is realized by a low-finesse intracavity etalon, with free spectral range $\Delta\omega_{\rm etal} = \omega_m/\alpha$ incommensurate with respect to the modulation frequency and much smaller than the gain bandwidth. The potential amplitude V_0 is determined by the reflectance R of etalon facets according to the relation $V_0 \simeq R$ (see Ref. [68] for technical details). The evolution of spectral amplitudes ψ_n at successive round-trips in the cavity is described by the coupled-mode equations of mode locking in frequency domain [68,72,74]

$$i\frac{d\psi_n}{dt} = J(\psi_{n+1} + \psi_{n-1}) + V_0\exp(2\pi i\alpha n + i\theta)\psi_n + i\mathcal{L}\psi_n, \tag{8}$$

where t is the round-trip number (i.e., physical time normalized to the cavity photon transit time) and $\mathcal{L}$ accounts for the effects of cavity losses and amplification in the gain medium. For a homogeneously broadened gain medium and neglecting other cavity dispersion effects, one can assume [70,72] $\mathcal{L} = -\gamma + g/(1 + 4n^2\omega_m^2/\Delta\omega_g^2)$, where γ is the effective loss rate of the cavity per round-trip, $n = 0$ is the index of the spectral axial mode at the center of the Lorentzian gainline, and g is the saturated gain. For a slow gain medium, g satisfies the rate equation [70]

$$dg/dt = \gamma_{\parallel}[g_0 - g(1 + I)], \tag{9}$$

where g_0 is the small-signal gain, $\gamma_{\parallel}$ is the relaxation rate of the population inversion normalized to the modulation frequency, and $I = \sum_n|\psi_n|^2$ is the intracavity laser intensity, averaged over the cavity round-trip time and normalized to the saturation intensity of the two-level transition. Clearly, in the limit of a broad gainline $\omega_m/\Delta\omega_g \to 0$ and assuming $g \simeq \gamma$, the spectral mode dynamics as described by Eq. (8) emulates the non-Hermitian AAH model. This means that, in the localized (insulating) phase $J < V_0$, a narrow laser spectrum, localized near the center of the gainline, should be observed, whereas a rather abrupt spectral broadening should arise in the delocalized (metallic) phase $J > V_0$. In the latter case the actual oscillating laser spectrum is ultimately limited by the finite bandwidth of the gain medium according to the Kuizenga-Siegman theory of active mode locking [71]. Figure 3 shows a typical behavior of laser spectra, as obtained after transient laser switch-on dynamics starting from random noise of spectral amplitudes, for increasing values of the FM modulation strength $\Delta_{\rm FM}$. Parameter values used in the simulation are typical for the Nd:YAG laser [68,71] and correspond to an incommensurate potential with $\alpha = (\sqrt{5} - 1)/4$ and $V_0 = 0.14$. The behavior of the oscillating bandwidth vs $\Delta_{\rm FM}$ [Fig. 3(a)] clearly shows an abrupt change at $\Delta_{\rm FM} \simeq 2V_0$, corresponding to the non-Hermitian topological phase transition from the insulating to the metallic phase.

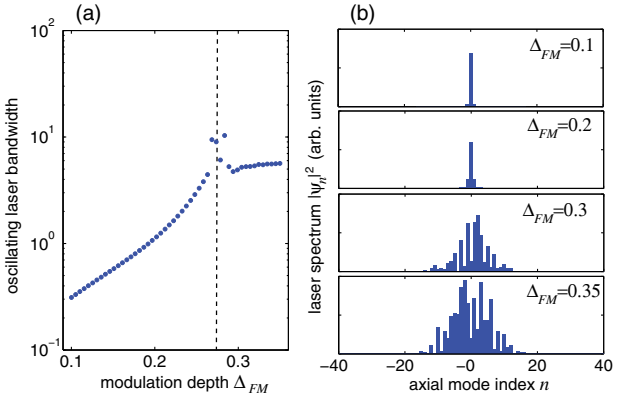

FIG. 3. Non-Hermitian phase transition in the spectrum of a FM mode-locked laser. (a) Behavior of the spectral width of the oscillating laser modes (in log scale), normalized to the modulation frequency, vs modulation depth $\Delta_{\rm FM}$. (b) Detailed profiles of laser spectra at a few increasing values of $\Delta_{\rm FM}$. The laser spectra are taken after transient relaxation oscillations by numerical simulations of Eqs. (8) and (9). Parameter values used in the simulations are: $\gamma = 0.19$, $g_0 = 3\gamma$, $\omega_m = 2\pi \times 1.384$ GHz, $\Delta\omega_g = 2\pi \times 126$ GHz, $\alpha = (\sqrt{5} - 1)/2$ and $V_0 = 0.14$. The dashed vertical curve in (a) corresponds to the critical value $\Delta_{FM} = 2V_0$ of the topological non-Hermitian phase transition.

Conclusions.—The discovery of topological phases in non-Hermitian open systems challenges the current wisdom of topological order. Recent studies have provided many insights to solve major issues such as generalizations of the bulk-boundary correspondence; however little is known about topological properties of non-Hermitian QCs.

Here we have considered a non-Hermitian extension of the Aubry-André-Harper model, and uncovered the topological nature of the non-Hermitian metal-insulator phase transition observed when the complex phase of the incommensurate potential is varied. A photonic realization of a non-Hermitian QC, which could provide a signature of the phase transition, has been also proposed. There are several open questions ahead. For example, the winding number in Eq. (5) uncovers the bulk topological nature of metallic or insulating phases of the QC, however, unlike the Hatano-Nelson crystal with open boundaries, showing the non-Hermitian skin effect [37], it is not useful to study edge states. Attempts to provide a topological classification of edge states in non-Hermitian QCs have been suggested very recently [77]. Finally, it would be interesting to extend the present study to other non-Hermitian QCs, such as Fibonacci chains and two-dimensional QCs.

*Corresponding author.
stefano.longhi@polimi.it

[1] M. Z. Hasan and C. L. Kane, Colloquium: Topological insulators, Rev. Mod. Phys. **82**, 3045 (2010).
[2] A. Bansil, H. Lin, and T. Das, Colloquium: Topological band theory, Rev. Mod. Phys. **88**, 021004 (2016).
[3] L. Lu, J. D. Joannopoulos, and M. Soljačić, Topological photonics, Nat. Photonics **8**, 821 (2014).
[4] N. Goldman, J. C. Budich, and P. Zoller, Topological quantum matter with ultracold gases in optical lattices, Nat. Phys. **12**, 639 (2016).
[5] T. Ozawa, H. M. Price, A. Amo, N. Goldman, M. Hafezi, L. Lu, M. Rechtsman, D. Schuster, J. Simon, O. Zilberberg, and I. Carusotto, Topological photonics, Rev. Mod. Phys. **91**, 015006 (2019).
[6] D.-W. Zhang, Y.-Q. Zhu, Y. X. Zhao, H. Yan, and S.-L. Zhu, Topological quantum matter with cold atoms, Adv. Phys. **67**, 253 (2018).
[7] Z. Yang, F. Gao, X. Shi, X. Lin, Z. Gao, Y. Chong, and B. Zhang, Topological Acoustics, Phys. Rev. Lett. **114**, 114301 (2015).
[8] S. D. Huber, Topological mechanics, Nat. Phys. **12**, 621 (2016).
[9] A. Altland and M. R. Zirnbauer, Nonstandard symmetry classes in mesoscopic normal-superconducting hybrid structures, Phys. Rev. B **55**, 1142 (1997).
[10] S. Ryu, A. P. Schnyder, A. Furusaki, and A. W. W. Ludwig, Topological insulators and superconductors: Tenfold way and dimensional hierarchy, New J. Phys. **12**, 065010 (2010).
[11] J. M. Zeuner, M. C. Rechtsman, Y. Plotnik, Y. Lumer, S. Nolte, M. S. Rudner, M. Segev, and A. Szameit, Observation of a Topological Transition in the Bulk of a Non-Hermitian System, Phys. Rev. Lett. **115**, 040402 (2015).
[12] C. Poli, M. Bellec, U. Kuhl, F. Mortessagne, and H. Schomerus, Selective enhancement of topologically induced interface states in a dielectric resonator chain, Nat. Commun. **6**, 6710 (2015).
[13] P. Peng, W. Cao, C. Shen, W. Qu, J. Wen, L. Jiang, and Y. Xiao, Anti-parity-time symmetry with flying atoms, Nat. Phys. **12**, 1139 (2016).
[14] H. Xu, D. Mason, L. Jiang, and J. G. E. Harris, Topological energy transfer in an optomechanical system with exceptional points, Nature (London) **537**, 80 (2016).
[15] S. Weimann, M. Kremer, Y. Plotnik, Y. Lumer, S. Nolte, K. G. Makris, M. Segev, M. C. Rechtsman, and A. Szameit, Topologically protected bound states in photonic parity-time-symmetric crystals, Nat. Mater. **16**, 433 (2017).
[16] M. Pan, H. Zhao, P. Miao, S. Longhi, and L. Feng, Photonic zero mode in a non-Hermitian photonic lattice, Nat. Commun. **9**, 1308 (2018).
[17] H. Zhou, C. Peng, Y. Yoon, C. W. Hsu, K. A. Nelson, L. Fu, J. D. Joannopoulos, M. Soljačić, and B. Zhen, Observation of bulk fermi arc and polarization half charge from paired exceptional points, Science **359**, 1009 (2018).
[18] N. Hatano and D. R. Nelson, Localization Transitions in Non-Hermitian Quantum Mechanics, Phys. Rev. Lett. **77**, 570 (1996).
[19] N. Hatano and D. R. Nelson, Vortex pinning and non-Hermitian quantum mechanics, Phys. Rev. B **56**, 8651 (1997).
[20] N. Hatano and D. R. Nelson, Non-Hermitian delocalization and eigenfunctions, Phys. Rev. B **58**, 8384 (1998).
[21] P. W. Brouwer, P. G. Silvestrov, and C. W. J. Beenakker, Theory of directed localization in one dimension, Phys. Rev. B **56**, R4333 (1997).
[22] M. S. Rudner and L. S. Levitov, Topological Transition in a Non-Hermitian Quantum Walk, Phys. Rev. Lett. **102**, 065703 (2009).
[23] K. Esaki, M. Sato, K. Hasebe, and M. Kohmoto, Edge states and topological phases in non-Hermitian systems, Phys. Rev. B **84**, 205128 (2011).
[24] H. Schomerus, Topologically protected midgap states in complex photonic lattices, Opt. Lett. **38**, 1912 (2013).
[25] C. Yuce, Topological phase in a non-Hermitian $\mathcal{PT}$ symmetric system, Phys. Lett. A **379**, 1213 (2015).
[26] S. Longhi, D. Gatti, and G. Della Valle, Robust light transport in non-Hermitian photonic lattices, Sci. Rep. **5**, 13376 (2015).
[27] T. E. Lee, Anomalous Edge State in a Non-Hermitian Lattice, Phys. Rev. Lett. **116**, 133903 (2016).
[28] D. Leykam, K. Y. Bliokh, C. Huang, Y. D. Chong, and F. Nori, Edge Modes, Degeneracies, and Topological Numbers in Non-Hermitian Systems, Phys. Rev. Lett. **118**, 040401 (2017).
[29] C. Yin, H. Jiang, L. Li, R. Lü, and S. Chen, Geometrical meaning of winding number and its characterization of topological phases in one-dimensional chiral non-Hermitian systems, Phys. Rev. A **97**, 052115 (2018).
[30] S. Yao, F. Song, and Z. Wang, Non-Hermitian Chern Bands, Phys. Rev. Lett. **121**, 136802 (2018).
[31] H. Shen, B. Zhen, and L. Fu, Topological Band Theory for Non-Hermitian Hamiltonians, Phys. Rev. Lett. **120**, 146402 (2018).
[32] V. M. Martinez Alvarez, J. E. Barrios Vargas, and L. E. F. Foa Torres, Non-Hermitian robust edge states in one dimension: Anomalous localization and eigenspace condensation at exceptional points, Phys. Rev. B **97**, 121401 (2018).

[33] S. Longhi, Non-Hermitian gauged topological laser arrays, Ann. Phys. (Amsterdam) **530**, 1800023 (2018).

[34] C. Yuce and Z. Oztas, $\mathcal{PT}$-symmetry protected non-Hermitian topological systems, Sci. Rep. **8**, 17416 (2018).

[35] K. Takata and M. Notomi, Photonic Topological Insulating Phase Induced Solely by Gain and Loss, Phys. Rev. Lett. **121**, 213902 (2018).

[36] F. K. Kunst, E. Edvardsson, J. C. Budich, and E. J. Bergholtz, Biorthogonal Bulk-Boundary Correspondence in Non-Hermitian Systems, Phys. Rev. Lett. **121**, 026808 (2018).

[37] Z. Gong, Y. Ashida, K. Kawabata, K. Takasan, S. Higashikawa, and M. Ueda, Topological Phases of Non-Hermitian Systems, Phys. Rev. X **8**, 031079 (2018).

[38] S. Yao and Z. Wang, Edge States and Topological Invariants of Non-Hermitian Systems, Phys. Rev. Lett. **121**, 086803 (2018).

[39] Y. Xiong, Why does bulk boundary correspondence fail in some non-Hermitian topological models, J. Phys. Commun. **2**, 035043 (2018).

[40] K. Kawabata, K. Shiozaki, and M. Ueda, Non-Hermitian Chern Insulator, Phys. Rev. B **98**, 165148 (2018); A. Ghatak and T. Das, New topological invariants in non-Hermitian systems, J. Phys. Condens. Matter **31**, 263001 (2019); D. S. Borgnia, A. J. Kruchkov, and R.-J. Slagerhttps, Non-Hermitian boundary modes, arXiv:1902.07217.

[41] S. Longhi, Tight-binding lattices with an oscillating imaginary gauge field, Phys. Rev. A **94**, 022102 (2016).

[42] P. G. Harper, Single band motion of conduction electrons in a uniform magnetic field, Proc. Phys. Soc. London Sect. A **68**, 874 (1955).

[43] S. Aubry and G. André, Analyticity breaking and Anderson localization in incommensurate lattices, Ann. Isr. Phys. Soc. **3**, 133 (1980).

[44] J. B. Sokoloff, Unusual band structure, wave function and electrical conductance in crystals with incommensurate periodic potentials, Phys. Rep. **126**, 189 (1984).

[45] G. Roati, C. D'Errico, L. Fallani, M. Fattori, C. Fort, M. Zaccanti, G. Modugno, M. Modugno, and M. Inguscio, Anderson localization of a non-interacting Bose-Einstein condensate, Nature (London) **453**, 895 (2008).

[46] Y. Lahini, R. Pugatch, F. Pozzi, M. Sorel, R. Morandotti, N. Davidson, and Y. Silberberg, Observation of a Localization Transition in Quasiperiodic Photonic Lattices, Phys. Rev. Lett. **103**, 013901 (2009).

[47] Y. E. Kraus, Y. Lahini, Z. Ringel, M. Verbin, and O. Zilberberg, Topological States and Adiabatic Pumping in Quasicrystals, Phys. Rev. Lett. **109**, 106402 (2012).

[48] L.-J. Lang, X. Cai, and S. Chen, Edge States and Topological Phases in One-Dimensional Optical Superlattices, Phys. Rev. Lett. **108**, 220401 (2012).

[49] S. Ganeshan, K. Sun, and S. Das Sarma, Topological Zero-Energy Modes in Gapless Commensurate Aubry-André-Harper Models, Phys. Rev. Lett. **110**, 180403 (2013).

[50] M. Verbin, O. Zilberberg, Y. E. Kraus, Y. Lahini, and Y. Silberberg, Observation of Topological Phase Transitions in Photonic Quasicrystals, Phys. Rev. Lett. **110**, 076403 (2013).

[51] S. Longhi, $\mathcal{PT}$-symmetric optical superlattices, J. Phys. A **47**, 165302 (2014).

[52] C. Yuce, $\mathcal{PT}$-symmetric Aubry-André model, Phys. Lett. A **378**, 2024 (2014).

[53] C. H. Liang, D. D. Scott, and Y. N. Joglekar, $\mathcal{PT}$ restoration via increased loss-gain in $\mathcal{PT}$ -symmetric Aubry-André model, Phys. Rev. A **89**, 030102 (2014).

[54] C. Hang, Y. V. Kartashov, G. Huang, and V. V. Konotop, Localization of light in a parity-time-symmetric quasiperiodic lattice, Opt. Lett. **40**, 2758 (2015).

[55] A. K. Harter, T. E. Lee, and Y. N. Joglekar, $\mathcal{PT}$-breaking threshold in spatially asymmetric Aubry-Andrè and Harper models: Hidden symmetry and topological states, Phys. Rev. A **93**, 062101 (2016).

[56] Q.-B. Zeng, S. Chen, and R. Lü, Anderson localization in the Non-Hermitian Aubry-André-Harper model with physical gain and loss, Phys. Rev. A **95**, 062118 (2017).

[57] S. Ostlund and R. Pandit, Renormalization-group analysis of the discrete quasiperiodic Schrodinger equation, Phys. Rev. B **29**, 1394 (1984).

[58] A. Avila and S. Jitomirskaya, The ten martini problem, Ann. Math. **170**, 303 (2009).

[59] R. B. Diener, G. A. Georgakis, J. Zhong, M. Raizen, and Q. Niu, Transition between extended and localized states in a one-dimensional incommensurate optical lattice, Phys. Rev. A **64**, 033416 (2001).

[60] K. A. Madsen, E. J. Bergholtz, and P. W. Brouwer, Topological equivalence of crystal and quasicrystal band structures, Phys. Rev. B **88**, 125118 (2013).

[61] Y. E. Kraus, Z. Ringel, and O. Zilberberg, Comment on Topological equivalence of crystal and quasicrystal band structures, arXiv:1308.2378v1.

[62] Y. E. Kraus, Z. Ringel, and O. Zilberberg, Four-Dimensional Quantum Hall Effect in a Two-Dimensional Quasicrystal, Phys. Rev. Lett. **111**, 226401 (2013).

[63] D.-T. Tran, A. Dauphin, N. Goldman, and P. Gaspard, Topological Hofstadter insulators in a two-dimensional quasicrystal, Phys. Rev. B **91**, 085125 (2015).

[64] E. Prodan, Virtual topological insulators with real quantized physics, Phys. Rev. B **91**, 245104 (2015).

[65] M. A. Bandres, M. C. Rechtsman, and M. Segev, Topological Photonic Quasicrystals: Fractal Topological Spectrum and Protected Transport, Phys. Rev. X **6**, 011016 (2016).

[66] Y. E. Kraus and O. Zilberberg, Quasiperiodicity and topology transcend dimensions, Nat. Phys. **12**, 624 (2016).

[67] D. J. Thouless, Quantization of particle transport, Phys. Rev. B **27**, 6083 (1983).

[68] See Supplemental Material at http://link.aps.org/supplemental/10.1103/PhysRevLett.122.237601 for technical details regarding the following: (i) Metal-insulator phase transition, $\mathcal{PT}$ symmetry breaking and winding number calculations; (ii) Eedge effects; (iii) photonic implementation of a non-Hermitian quasicrystal.

[69] D. J. Thouless, A relation between the density of states and range of localization for one dimensional random systems, J. Phys. C **5**, 77 (1972).

[70] D. J. Kuizenga and A. E. Siegman, FM and AM mode locking of the homogeneous laser-part I, IEEE J. Quantum Electron. **6**, 694 (1970).

[71] D. J. Kuizenga and A. E. Siegman, FM and AM mode locking of the homogeneous laser-part II, IEEE J. Quantum Electron. **6**, 709 (1970).

[72] H. A. Haus, Mode-locking of lasers, IEEE J. Sel. Top. Quantum Electron. **6**, 1173 (2000).

[73] B. Fischer, B. Vodonos, S. Atkins, and A. Bekker, Experimental demonstration of localization in the frequency domain of mode-locked lasers with dispersion, Opt. Lett. **27**, 1061 (2002).

[74] A. Gordon and B. Fischer, Statistical-mechanics theory of active mode locking with noise, Opt. Lett. **29**, 1022 (2004).

[75] S. Longhi, Metal-insulator transition in the spectrum of a frequency-modulation mode-locked laser, Phys. Rev. A **77**, 015807 (2008).

[76] A. Rosen, R. Weill, B. Levit, V. Smulakovsky, A. Bekker, and B. Fischer, Experimental Observation of Critical Phenomena in a Laser Light System, Phys. Rev. Lett. **105**, 013905 (2010).

[77] Q.-B. Zeng, Y.-B. Yang, and Y. Xu, Topological Non-Hermitian Quasicrystals, arXiv:1901.08060v1.